

# **Effective Integration of BCS with the IMSA to Enhance the Microwave Imaging of Sparse Objects Under the Born Approximation**

N. Anselmi, L. Poli, G. Oliveri, and A. Massa

## **Abstract**

In this work, the microwave imaging of sparse scatterers under the first order Born approximation is dealt with. Towards this end, an innovative Bayesian compressive sensing (*BCS*) methodology is derived and implemented in order to combine the well-known regularization capabilities of *CS* solvers with the progressively acquired information about the imaged scenario through the iterative multi-scaling approach (*IMSA*).

Selected numerical results are presented in order to verify the effectiveness of the proposed *IMSA-BCS* technique, as well as to compare it against competitive state-of-the-art approaches.

# 1 Numerical Results

## 1.1 E-shaped Object, $\ell = 1.5\lambda$

### Test Case Description

#### Direct solver:

- Side of the investigation domain:  $L = 6.0\lambda$
- Cubic domain divided in  $\sqrt{D} \times \sqrt{D}$  cells
- Number of cells for the direct solver:  $D = 1600$  (discretization =  $\lambda/10$ )

#### Investigation domain:

- Cubic domain divided in  $\sqrt{N} \times \sqrt{N}$  cells
- Number of cells for the inversion:
  - First Step IMSA:  $N^{(1)} = 100$  (discretization =  $\lambda/10$ )
  - Following Steps IMSA:  $N^{(i)}$  not fixed, defined according to the estimated *RoI*  $\mathcal{D}^{(i)}$

#### Measurement domain:

- Total number of measurements:  $M = 60$
- Measurement points placed on circles of radius  $\rho = 4.5\lambda$

#### Sources:

- Plane waves
- Number of views:  $V = 60$ ;  $\theta_{inc}^v = 0^\circ + (v - 1) \times (360/V)$
- Amplitude:  $A = 1.0$
- Frequency:  $F = 300$  MHz ( $\lambda = 1$ )

#### Background:

- $\epsilon_r = 1.0$
- $\sigma = 0$  [S/m]

#### Scatterer

- E-shaped object,  $\ell = 1.5\lambda$
- $\epsilon_r \in \{1.01, 1.02, 1.04, 1.05, 1.06, 1.08, 1.10, 1.15, 1.20\}$
- $\sigma = 0$  [S/m]

### 1.1.1 E-shaped Object, $\ell = 1.5\lambda$ , $\tau = 0.02$ - IMSA - BCS vs. TVCS vs. BP reconstructed profiles

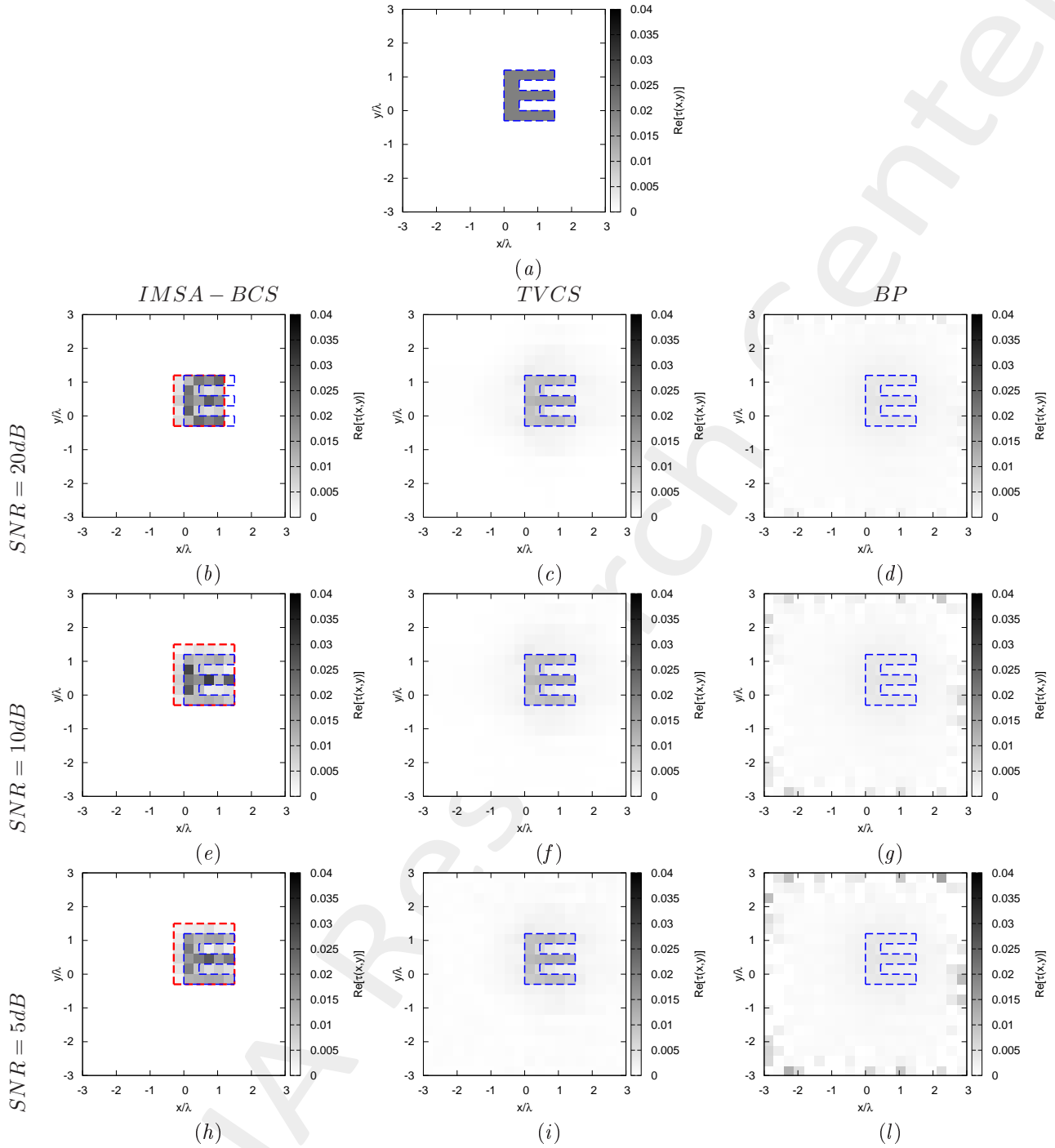


Figure 1: *E-shaped Object,  $\ell = 1.5\lambda$ ,  $\tau = 0.02$  - IMSA-BCS vs. TVCS vs. BP* - (a) Actual profile, (b)(e)(h) IMSA-BCS, (c)(f)(i) TVCS and (d)(g)(l) BP reconstructed profiles for (b)(c)(d) SNR = 20 [dB], (e)(f)(g) SNR = 10 [dB] and (h)(i)(l) SNR = 5 [dB].

	$SNR = 50dB$		
	$IMSA - BCS$	$TVCS$	$BP$
$\xi_{tot}$	$5.12 \times 10^{-4}$	$9.10 \times 10^{-4}$	$1.53 \times 10^{-3}$
$\xi_{int}$	$7.76 \times 10^{-3}$	$9.71 \times 10^{-3}$	$1.57 \times 10^{-2}$
$\xi_{ext}$	$1.71 \times 10^{-4}$	$4.95 \times 10^{-4}$	$8.64 \times 10^{-4}$
	$SNR = 20dB$		
	$IMSA - BCS$	$TVCS$	$BP$
$\xi_{tot}$	$4.53 \times 10^{-4}$	$9.17 \times 10^{-4}$	$1.65 \times 10^{-3}$
$\xi_{int}$	$6.70 \times 10^{-3}$	$9.64 \times 10^{-3}$	$1.57 \times 10^{-2}$
$\xi_{ext}$	$1.56 \times 10^{-4}$	$5.06 \times 10^{-4}$	$9.27 \times 10^{-4}$
	$SNR = 10dB$		
	$IMSA - BCS$	$TVCS$	$BP$
$\xi_{tot}$	$5.53 \times 10^{-4}$	$1.00 \times 10^{-3}$	$2.14 \times 10^{-3}$
$\xi_{int}$	$8.04 \times 10^{-3}$	$9.94 \times 10^{-3}$	$1.57 \times 10^{-2}$
$\xi_{ext}$	$1.99 \times 10^{-4}$	$5.81 \times 10^{-4}$	$1.25 \times 10^{-3}$
	$SNR = 5dB$		
	$IMSA - BCS$	$TVCS$	$BP$
$\xi_{tot}$	$4.37 \times 10^{-4}$	$1.18 \times 10^{-3}$	$2.74 \times 10^{-3}$
$\xi_{int}$	$5.40 \times 10^{-3}$	$9.96 \times 10^{-3}$	$1.57 \times 10^{-2}$
$\xi_{ext}$	$2.01 \times 10^{-4}$	$7.69 \times 10^{-4}$	$1.68 \times 10^{-3}$

Table I: *E-shaped Object*,  $\ell = 1.5\lambda$ ,  $\tau = 0.02$  - *IMSA-BCS* vs. *TVCS* vs. *BP* - Reconstruction errors: total ( $\xi_{tot}$ ), internal ( $\xi_{int}$ ) and external ( $\xi_{ext}$ ) errors.

### 1.1.2 E-shaped Object, $\ell = 1.5\lambda$ , $\tau = 0.05$ - IMSA-BCS vs. TVCS vs. BP reconstructed profiles

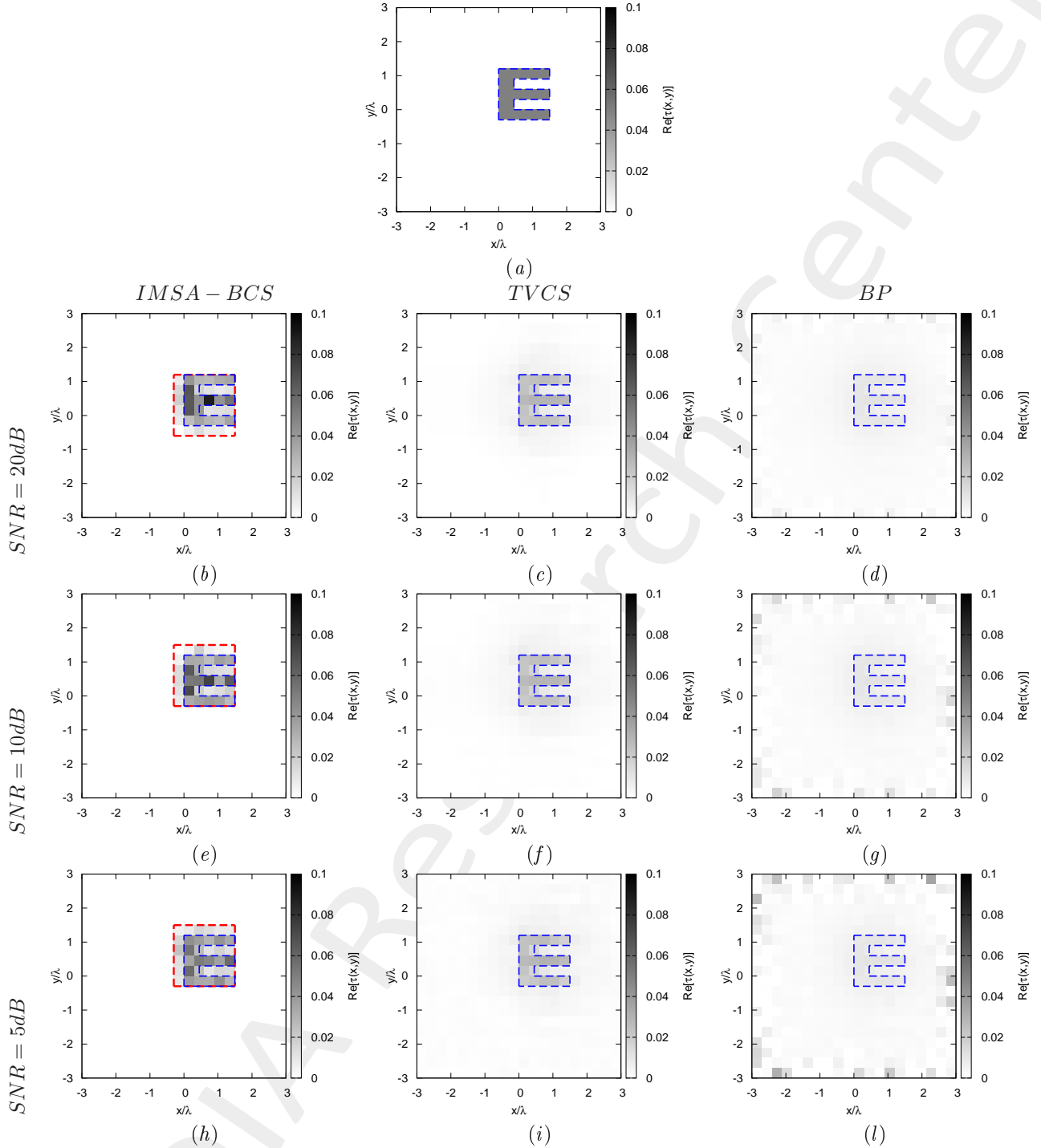


Figure 2: *E-shaped Object,  $\ell = 1.5\lambda$ ,  $\tau = 0.05$  - IMSA-BCS vs. TVCS vs. BP* - (a) Actual profile, (b)(e)(h) IMSA-BCS, (c)(f)(i) TVCS and (d)(g)(l) BP reconstructed profiles for (b)(c)(d) SNR = 20 [dB], (e)(f)(g) SNR = 10 [dB] and (h)(i)(l) SNR = 5 [dB].

	$SNR = 50dB$		
	$IMSA - BCS$	$TVCS$	$BP$
$\xi_{tot}$	$1.18 \times 10^{-3}$	$2.29 \times 10^{-3}$	$3.78 \times 10^{-3}$
$\xi_{int}$	$1.54 \times 10^{-2}$	$2.38 \times 10^{-2}$	$3.82 \times 10^{-2}$
$\xi_{ext}$	$4.92 \times 10^{-4}$	$1.27 \times 10^{-3}$	$2.15 \times 10^{-3}$
	$SNR = 20dB$		
	$IMSA - BCS$	$TVCS$	$BP$
$\xi_{tot}$	$1.25 \times 10^{-3}$	$2.30 \times 10^{-3}$	$4.09 \times 10^{-3}$
$\xi_{int}$	$1.64 \times 10^{-2}$	$2.41 \times 10^{-2}$	$3.82 \times 10^{-2}$
$\xi_{ext}$	$5.15 \times 10^{-4}$	$1.27 \times 10^{-3}$	$2.31 \times 10^{-3}$
	$SNR = 10dB$		
	$IMSA - BCS$	$TVCS$	$BP$
$\xi_{tot}$	$1.20 \times 10^{-3}$	$2.55 \times 10^{-3}$	$5.29 \times 10^{-3}$
$\xi_{int}$	$1.52 \times 10^{-2}$	$2.49 \times 10^{-2}$	$3.82 \times 10^{-2}$
$\xi_{ext}$	$5.25 \times 10^{-4}$	$1.50 \times 10^{-3}$	$3.12 \times 10^{-3}$
	$SNR = 5dB$		
	$IMSA - BCS$	$TVCS$	$BP$
$\xi_{tot}$	$1.14 \times 10^{-3}$	$2.91 \times 10^{-3}$	$6.80 \times 10^{-3}$
$\xi_{int}$	$1.10 \times 10^{-2}$	$2.46 \times 10^{-2}$	$3.83 \times 10^{-2}$
$\xi_{ext}$	$6.34 \times 10^{-4}$	$1.88 \times 10^{-3}$	$4.18 \times 10^{-3}$

Table II: *E-shaped Object*,  $\ell = 1.5\lambda$ ,  $\tau = 0.05$  - *IMSA-BCS vs. TVCS vs. BP* - Reconstruction errors: total ( $\xi_{tot}$ ), internal ( $\xi_{int}$ ) and external ( $\xi_{ext}$ ) errors.

### 1.1.3 E-shaped Object, $\ell = 1.5\lambda$ , $\tau = 0.15$ - IMSA-BCS vs. TVCS vs. BP reconstructed profiles

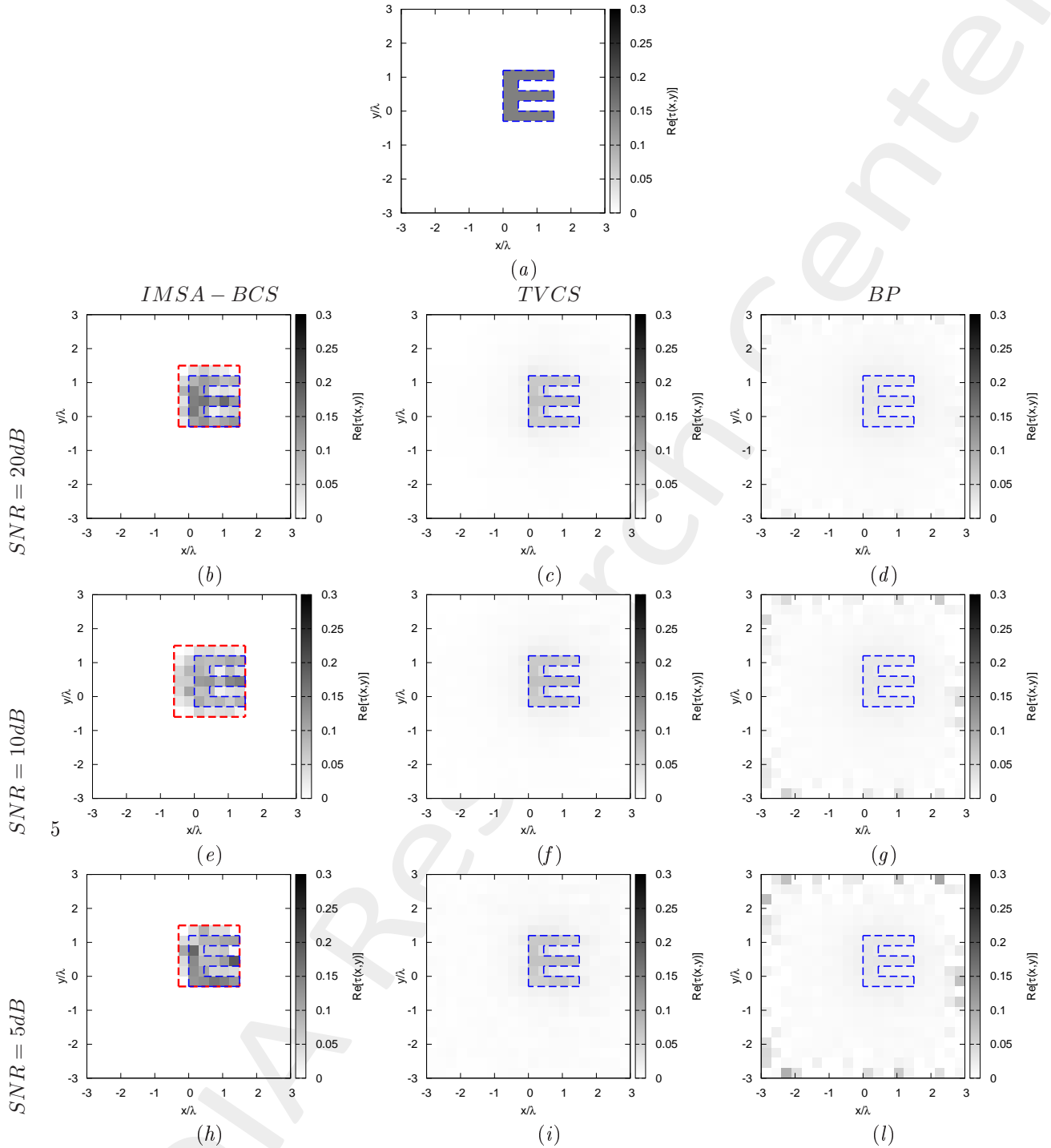


Figure 3: *E-shaped Object,  $\ell = 1.5\lambda$ ,  $\tau = 0.15$  - IMSA-BCS vs. TVCS vs. BP* - (a) Actual profile, (b)(e)(h) IMSA-BCS, (c)(f)(i) TVCS and (d)(g)(l) BP reconstructed profiles for (b)(c)(d) SNR = 20 [dB], (e)(f)(g) SNR = 10 [dB] and (h)(i)(l) SNR = 5 [dB].

	$SNR = 50dB$		
	$IMSA - BCS$	$TVCS$	$BP$
$\xi_{tot}$	$4.03 \times 10^{-3}$	$7.41 \times 10^{-3}$	$1.09 \times 10^{-2}$
$\xi_{int}$	$4.09 \times 10^{-2}$	$7.25 \times 10^{-2}$	$1.06 \times 10^{-1}$
$\xi_{ext}$	$1.78 \times 10^{-3}$	$4.34 \times 10^{-3}$	$6.24 \times 10^{-3}$
	$SNR = 20dB$		
	$IMSA - BCS$	$TVCS$	$BP$
$\xi_{tot}$	$3.80 \times 10^{-3}$	$7.50 \times 10^{-3}$	$1.18 \times 10^{-2}$
$\xi_{int}$	$3.13 \times 10^{-2}$	$7.48 \times 10^{-2}$	$1.06 \times 10^{-1}$
$\xi_{ext}$	$1.89 \times 10^{-3}$	$4.33 \times 10^{-3}$	$6.70 \times 10^{-3}$
	$SNR = 10dB$		
	$IMSA - BCS$	$TVCS$	$BP$
$\xi_{tot}$	$5.61 \times 10^{-3}$	$8.12 \times 10^{-3}$	$1.53 \times 10^{-2}$
$\xi_{int}$	$4.88 \times 10^{-2}$	$7.52 \times 10^{-2}$	$1.06 \times 10^{-1}$
$\xi_{ext}$	$3.11 \times 10^{-3}$	$4.96 \times 10^{-3}$	$9.09 \times 10^{-3}$
	$SNR = 5dB$		
	$IMSA - BCS$	$TVCS$	$BP$
$\xi_{tot}$	$4.67 \times 10^{-3}$	$9.24 \times 10^{-3}$	$1.97 \times 10^{-2}$
$\xi_{int}$	$3.57 \times 10^{-2}$	$7.55 \times 10^{-2}$	$1.06 \times 10^{-1}$
$\xi_{ext}$	$2.18 \times 10^{-3}$	$6.11 \times 10^{-3}$	$1.21 \times 10^{-2}$

Table III: *E-shaped Object*,  $\ell = 1.5\lambda$ ,  $\tau = 0.15$  - *IMSA-BCS vs. TVCS vs. BP* - Reconstruction errors: total ( $\xi_{tot}$ ), internal ( $\xi_{int}$ ) and external ( $\xi_{ext}$ ) errors.

#### 1.1.4 E-shaped Object, $\ell = 1.5\lambda$ , $\tau = 0.20$ - IMSA-BCS vs. TVCS vs. BP reconstructed profiles

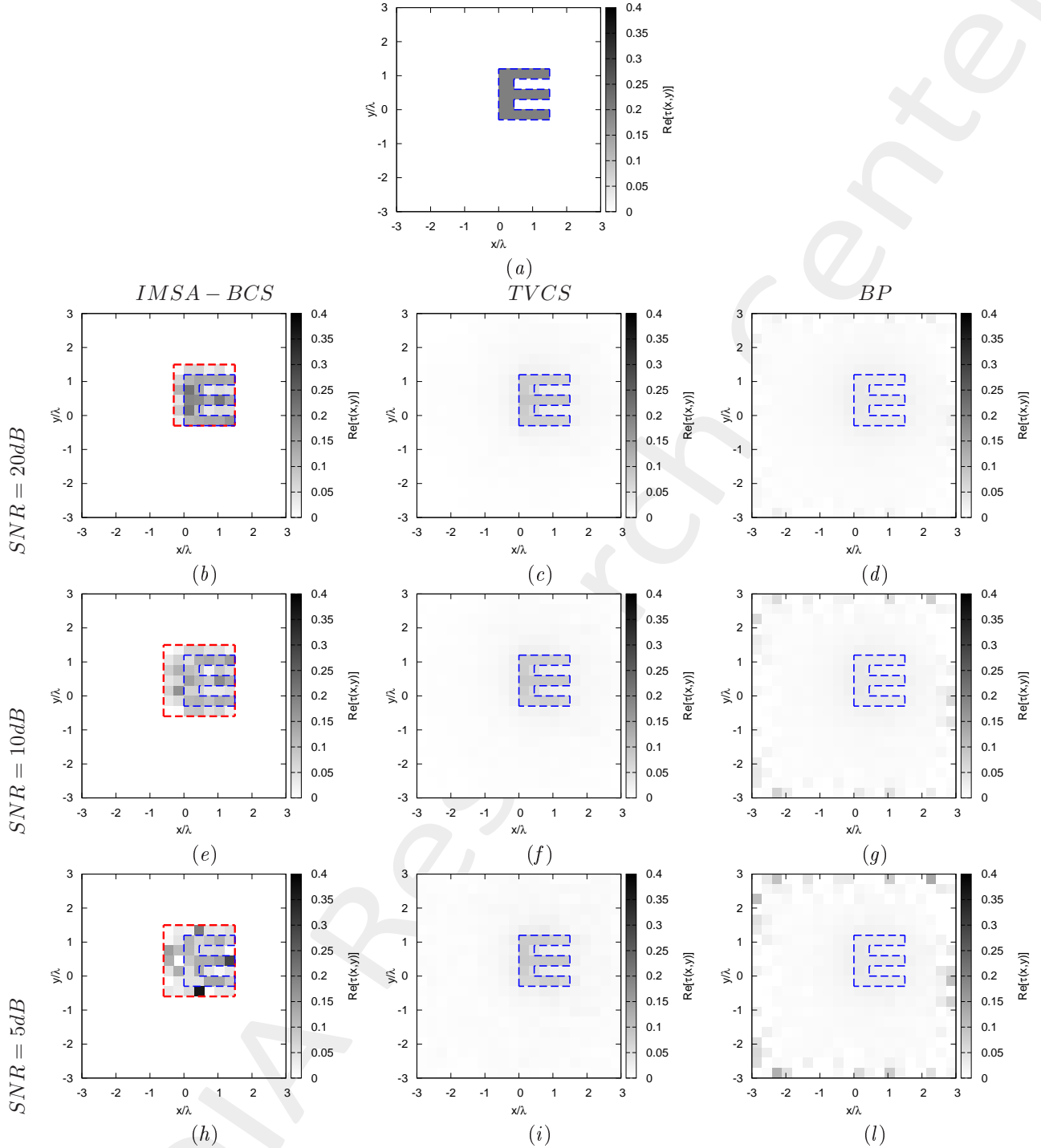


Figure 4: *E-shaped Object,  $\ell = 1.5\lambda$ ,  $\tau = 0.20$  - IMSA-BCS vs. TVCS vs. BP* - (a) Actual profile, (b)(e)(h) IMSA-BCS, (c)(f)(i) TVCS and (d)(g)(l) BP reconstructed profiles for (b)(c)(d) SNR = 20 [dB], (e)(f)(g) SNR = 10 [dB] and (h)(i)(l) SNR = 5 [dB].

	$SNR = 50dB$		
	$IMSA - BCS$	$TVCS$	$BP$
$\xi_{tot}$	$5.14 \times 10^{-3}$	$1.02 \times 10^{-2}$	$1.43 \times 10^{-2}$
$\xi_{int}$	$4.33 \times 10^{-2}$	$1.01 \times 10^{-1}$	$1.37 \times 10^{-1}$
$\xi_{ext}$	$2.23 \times 10^{-3}$	$5.96 \times 10^{-3}$	$8.07 \times 10^{-3}$
	$SNR = 20dB$		
	$IMSA - BCS$	$TVCS$	$BP$
$\xi_{tot}$	$5.42 \times 10^{-3}$	$1.04 \times 10^{-2}$	$1.54 \times 10^{-2}$
$\xi_{int}$	$4.39 \times 10^{-2}$	$1.01 \times 10^{-1}$	$1.37 \times 10^{-1}$
$\xi_{ext}$	$2.52 \times 10^{-3}$	$6.11 \times 10^{-3}$	$8.69 \times 10^{-3}$
	$SNR = 10dB$		
	$IMSA - BCS$	$TVCS$	$BP$
$\xi_{tot}$	$8.31 \times 10^{-3}$	$1.12 \times 10^{-2}$	$2.00 \times 10^{-2}$
$\xi_{int}$	$7.27 \times 10^{-2}$	$1.03 \times 10^{-1}$	$1.37 \times 10^{-1}$
$\xi_{ext}$	$4.44 \times 10^{-3}$	$6.89 \times 10^{-3}$	$1.18 \times 10^{-2}$
	$SNR = 5dB$		
	$IMSA - BCS$	$TVCS$	$BP$
$\xi_{tot}$	$1.15 \times 10^{-2}$	$1.27 \times 10^{-2}$	$2.58 \times 10^{-2}$
$\xi_{int}$	$8.38 \times 10^{-2}$	$1.03 \times 10^{-1}$	$1.37 \times 10^{-1}$
$\xi_{ext}$	$5.40 \times 10^{-3}$	$8.46 \times 10^{-3}$	$1.59 \times 10^{-2}$

Table IV: *E-shaped Object*,  $\ell = 1.5\lambda$ ,  $\tau = 0.20$  - *IMSA-BCS vs. TVCS vs. BP* - Reconstruction errors: total ( $\xi_{tot}$ ), internal ( $\xi_{int}$ ) and external ( $\xi_{ext}$ ) errors.

### 1.1.5 E-shaped Object, $\ell = 1.5\lambda$ - IMSA - BCS vs. TVCS vs. BP errors resume vs. $\tau$

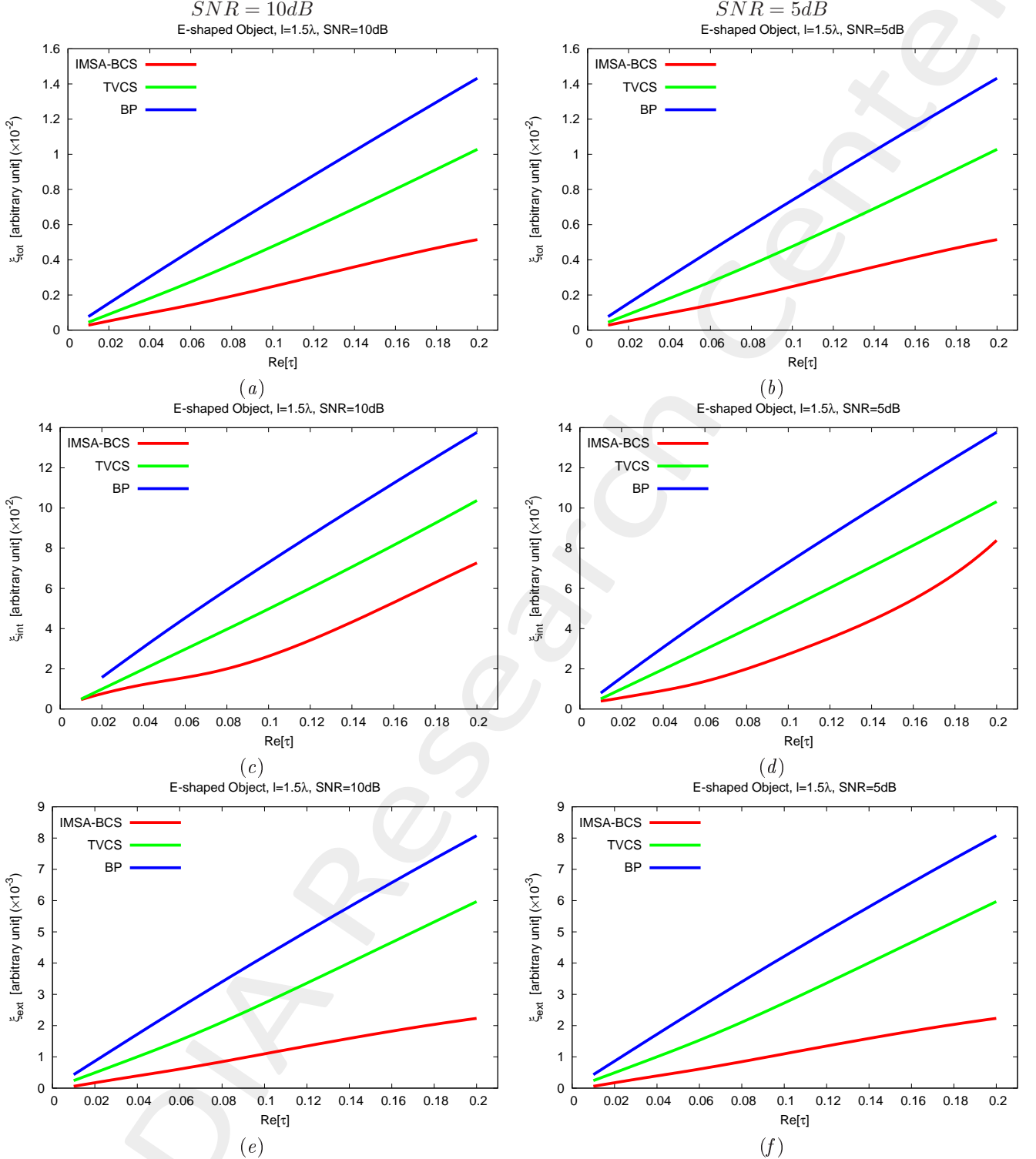


Figure 5: *E-shaped Object,  $\ell = 1.5\lambda$*  - Reconstruction errors vs.  $\tau$ : (a) total error, (b) internal error and (c) external error. Reconstruction errors vs.  $\tau$ : (a)(b) total error, (c)(d) internal error and (e)(f) external error for (a)(c)(e)  $\text{SNR} = 10 \text{ dB}$  and (b)(d)(f)  $\text{SNR} = 5 \text{ dB}$ .

## 1.2 Rhombus, $D = 1.5\lambda$

### Test Case Description

#### Direct solver:

- Side of the investigation domain:  $L = 6.0\lambda$
- Cubic domain divided in  $\sqrt{D} \times \sqrt{D}$  cells
- Number of cells for the direct solver:  $D = 1600$  (discretization =  $\lambda/10$ )

#### Investigation domain:

- Cubic domain divided in  $\sqrt{N} \times \sqrt{N}$  cells
- Number of cells for the inversion:
  - First Step IMSA:  $N^{(1)} = 100$  (discretization =  $\lambda/10$ )
  - Following Steps IMSA:  $N^{(i)}$  not fixed, defined according to the estimated *RoI*  $\mathcal{D}^{(i)}$

#### Measurement domain:

- Total number of measurements:  $M = 60$
- Measurement points placed on circles of radius  $\rho = 4.5\lambda$

#### Sources:

- Plane waves
- Number of views:  $V = 60$ ;  $\theta_{inc}^v = 0^\circ + (v - 1) \times (360/V)$
- Amplitude:  $A = 1.0$
- Frequency:  $F = 300$  MHz ( $\lambda = 1$ )

#### Background:

- $\epsilon_r = 1.0$
- $\sigma = 0$  [S/m]

#### Scatterer

- Rhombus,  $D = 1.5\lambda$
- $\epsilon_r \in \{1.01, 1.02, 1.04, 1.05, 1.06, 1.08, 1.10, 1.15, 1.20\}$
- $\sigma = 0$  [S/m]

### 1.2.1 Rhombus, $D = 1.5\lambda$ , $\tau = 0.02$ - IMSA - BCS vs. TVCS vs. BP reconstructed profiles

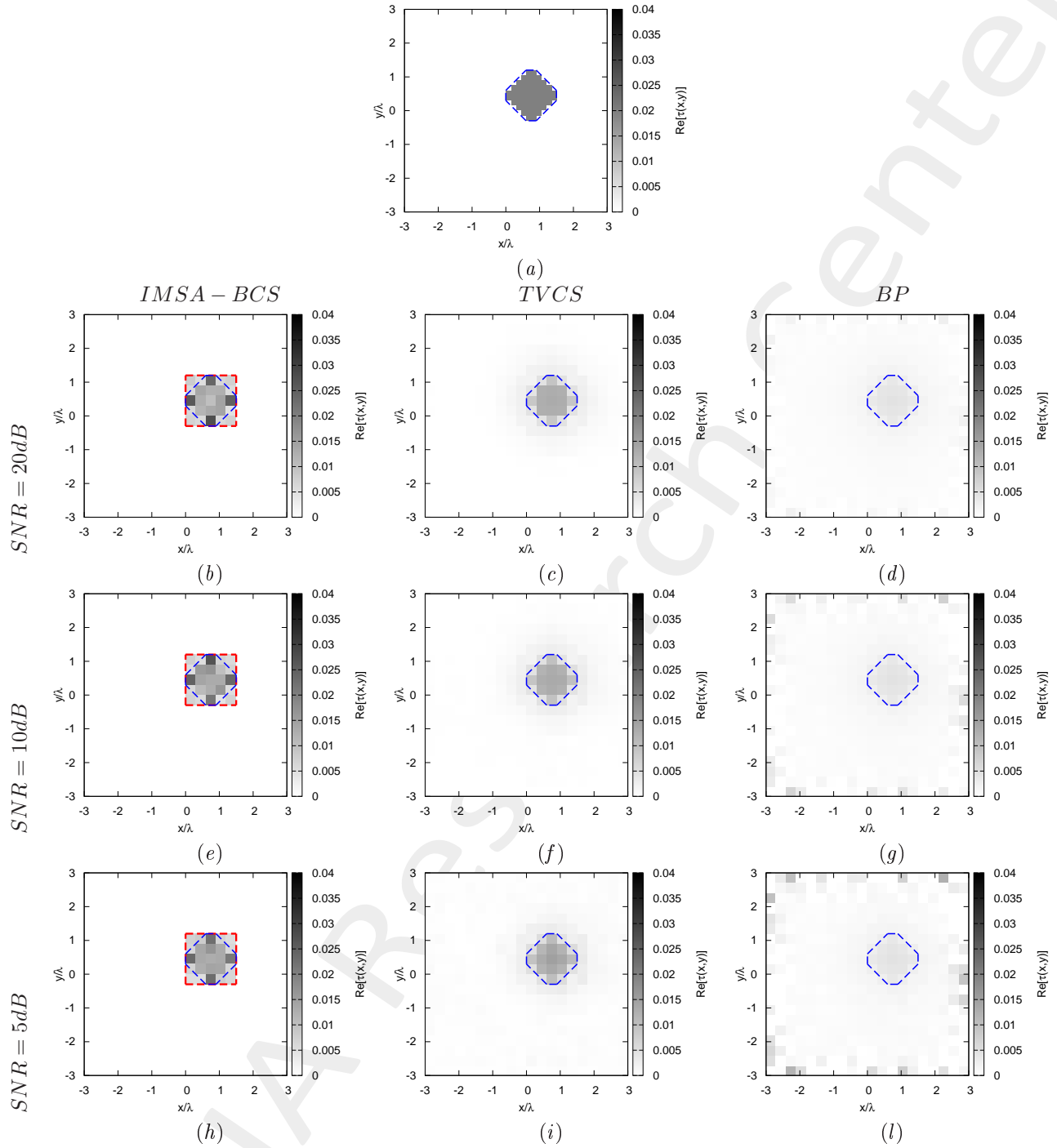


Figure 6: Rhombus,  $D = 1.5\lambda$ ,  $\tau = 0.02$  - IMSA-BCS vs. TVCS vs. BP - (a) Actual profile, (b)(e)(h)  $IMSA - BCS$ , (c)(f)(i)  $TVCS$  and (d)(g)(l)  $BP$  reconstructed profiles for (b)(c)(d)  $SNR = 20$  [dB], (e)(f)(g)  $SNR = 10$  [dB] and (h)(i)(l)  $SNR = 5$  [dB].

	$SNR = 50dB$		
	$IMSA - BCS$	$TVCS$	$BP$
$\xi_{tot}$	$4.48 \times 10^{-4}$	$7.59 \times 10^{-4}$	$1.28 \times 10^{-3}$
$\xi_{int}$	$7.80 \times 10^{-3}$	$9.47 \times 10^{-3}$	$1.58 \times 10^{-2}$
$\xi_{ext}$	$1.62 \times 10^{-4}$	$4.19 \times 10^{-4}$	$7.20 \times 10^{-4}$
	$SNR = 20dB$		
	$IMSA - BCS$	$TVCS$	$BP$
$\xi_{tot}$	$4.44 \times 10^{-4}$	$7.59 \times 10^{-4}$	$1.40 \times 10^{-3}$
$\xi_{int}$	$7.59 \times 10^{-3}$	$9.17 \times 10^{-3}$	$1.58 \times 10^{-2}$
$\xi_{ext}$	$1.66 \times 10^{-4}$	$4.31 \times 10^{-4}$	$7.82 \times 10^{-4}$
	$SNR = 10dB$		
	$IMSA - BCS$	$TVCS$	$BP$
$\xi_{tot}$	$4.04 \times 10^{-4}$	$8.36 \times 10^{-4}$	$1.85 \times 10^{-3}$
$\xi_{int}$	$6.67 \times 10^{-3}$	$9.00 \times 10^{-3}$	$1.58 \times 10^{-2}$
$\xi_{ext}$	$1.59 \times 10^{-4}$	$5.18 \times 10^{-4}$	$1.09 \times 10^{-3}$
	$SNR = 5dB$		
	$IMSA - BCS$	$TVCS$	$BP$
$\xi_{tot}$	$3.88 \times 10^{-4}$	$9.70 \times 10^{-4}$	$2.42 \times 10^{-3}$
$\xi_{int}$	$6.03 \times 10^{-3}$	$8.61 \times 10^{-3}$	$1.58 \times 10^{-2}$
$\xi_{ext}$	$1.67 \times 10^{-4}$	$6.72 \times 10^{-4}$	$1.48 \times 10^{-3}$

Table V: *Rhombus*,  $D = 1.5\lambda$ ,  $\tau = 0.02$  - *IMSA-BCS* vs. *TVCS* vs. *BP* - Reconstruction errors: total ( $\xi_{tot}$ ), internal ( $\xi_{int}$ ) and external ( $\xi_{ext}$ ) errors.

### 1.2.2 Rhombus, $D = 1.5\lambda$ , $\tau = 0.05$ - IMSA - BCS vs. TVCS vs. BP reconstructed profiles

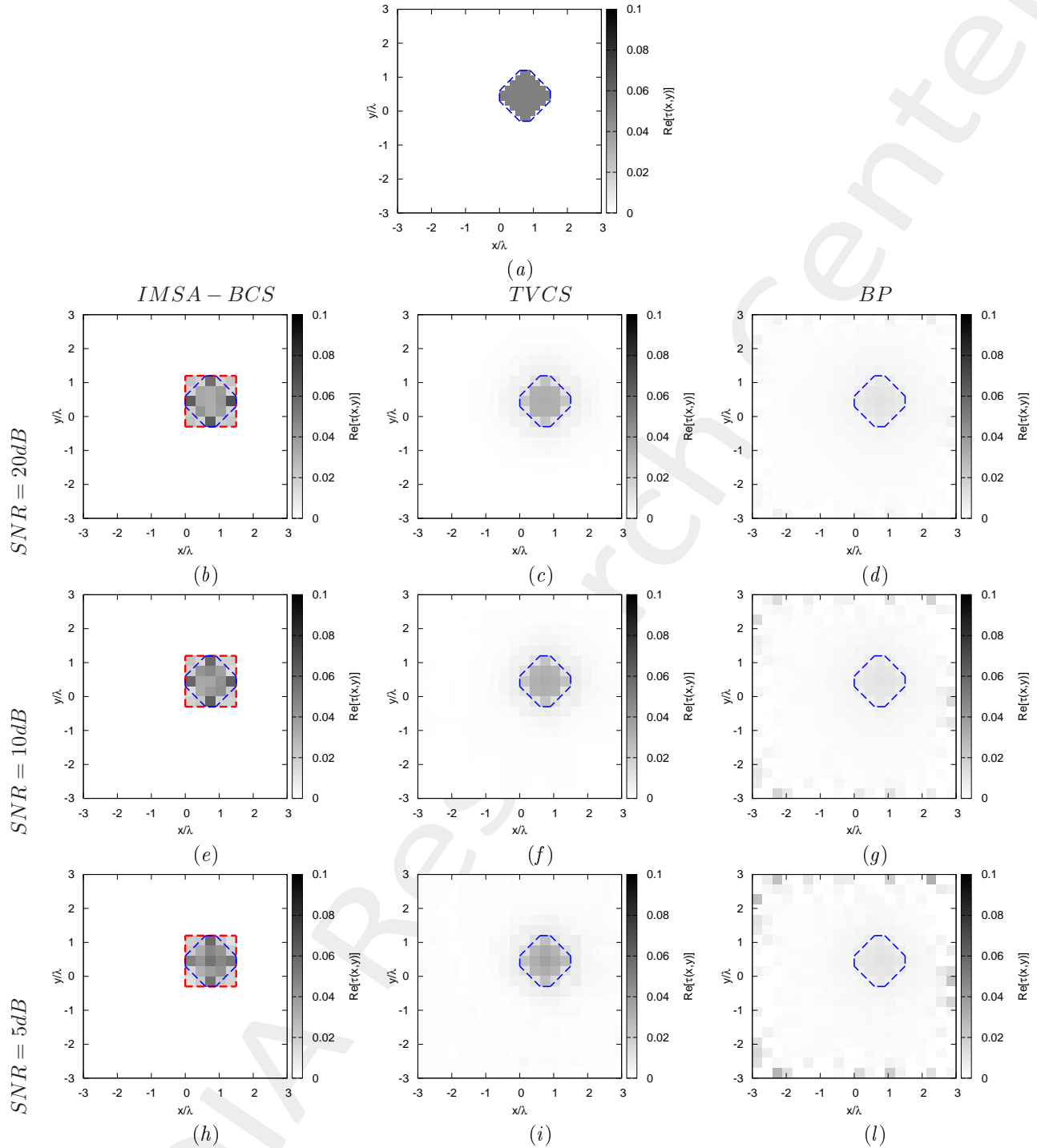


Figure 7: Rhombus,  $D = 1.5\lambda$ ,  $\tau = 0.05$  - IMSA-BCS vs. TVCS vs. BP - (a) Actual profile, (b)(e)(h) IMSA-BCS, (c)(f)(i) TVCS and (d)(g)(l) BP reconstructed profiles for (b)(c)(d)  $SNR = 20$  [dB], (e)(f)(g)  $SNR = 10$  [dB] and (h)(i)(l)  $SNR = 5$  [dB].

	$SNR = 50dB$		
	$IMSA - BCS$	$TVCS$	$BP$
$\xi_{tot}$	$1.12 \times 10^{-3}$	$1.91 \times 10^{-3}$	$2.55 \times 10^{-3}$
$\xi_{int}$	$1.65 \times 10^{-2}$	$2.28 \times 10^{-2}$	$3.11 \times 10^{-2}$
$\xi_{ext}$	$5.13 \times 10^{-4}$	$1.09 \times 10^{-3}$	$1.43 \times 10^{-3}$
	$SNR = 20dB$		
	$IMSA - BCS$	$TVCS$	$BP$
$\xi_{tot}$	$1.09 \times 10^{-3}$	$1.91 \times 10^{-3}$	$2.79 \times 10^{-3}$
$\xi_{int}$	$1.53 \times 10^{-2}$	$2.25 \times 10^{-2}$	$3.11 \times 10^{-2}$
$\xi_{ext}$	$5.27 \times 10^{-4}$	$1.10 \times 10^{-3}$	$1.56 \times 10^{-3}$
	$SNR = 10dB$		
	$IMSA - BCS$	$TVCS$	$BP$
$\xi_{tot}$	$9.67 \times 10^{-4}$	$2.12 \times 10^{-3}$	$3.69 \times 10^{-3}$
$\xi_{int}$	$1.30 \times 10^{-2}$	$2.26 \times 10^{-2}$	$3.11 \times 10^{-2}$
$\xi_{ext}$	$4.81 \times 10^{-4}$	$1.32 \times 10^{-3}$	$2.17 \times 10^{-3}$
	$SNR = 5dB$		
	$IMSA - BCS$	$TVCS$	$BP$
$\xi_{tot}$	$8.71 \times 10^{-4}$	$2.44 \times 10^{-3}$	$4.81 \times 10^{-3}$
$\xi_{int}$	$1.01 \times 10^{-2}$	$2.16 \times 10^{-2}$	$3.11 \times 10^{-2}$
$\xi_{ext}$	$4.74 \times 10^{-4}$	$1.69 \times 10^{-3}$	$2.96 \times 10^{-3}$

Table VI: *Rhombus*,  $D = 1.5\lambda$ ,  $\tau = 0.05$  - *IMSA-BCS* vs. *TVCS* vs. *BP* - Reconstruction errors: total ( $\xi_{tot}$ ), internal ( $\xi_{int}$ ) and external ( $\xi_{ext}$ ) errors.

### 1.2.3 Rhombus, $D = 1.5\lambda$ , $\tau = 0.10$ - IMSA - BCS vs. TVCS vs. BP reconstructed profiles

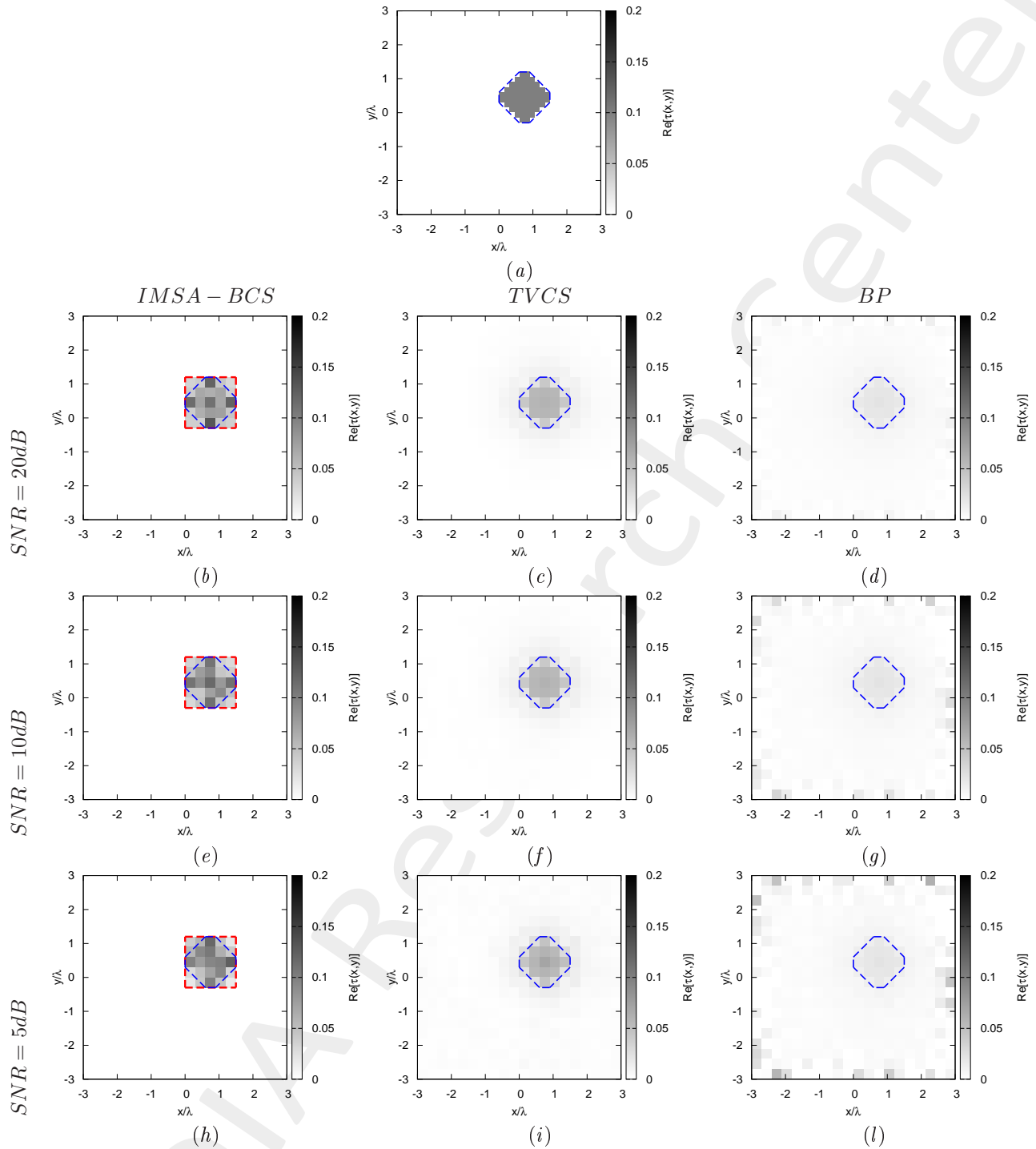


Figure 8: Rhombus,  $D = 1.5\lambda$ ,  $\tau = 0.02$  - IMSA-BCS vs. TVCS vs. BP - (a) Actual profile, (b)(e)(h) IMSA-BCS, (c)(f)(i) TVCS and (d)(g)(l) BP reconstructed profiles for (b)(c)(d)  $SNR = 20$  [dB], (e)(f)(g)  $SNR = 10$  [dB] and (h)(i)(l)  $SNR = 5$  [dB].

	$SNR = 50dB$		
	$IMSA - BCS$	$TVCS$	$BP$
$\xi_{tot}$	$2.10 \times 10^{-3}$	$3.89 \times 10^{-3}$	$6.23 \times 10^{-3}$
$\xi_{int}$	$2.72 \times 10^{-2}$	$4.62 \times 10^{-2}$	$7.40 \times 10^{-2}$
$\xi_{ext}$	$9.86 \times 10^{-4}$	$2.24 \times 10^{-3}$	$3.53 \times 10^{-3}$
	$SNR = 20dB$		
	$IMSA - BCS$	$TVCS$	$BP$
$\xi_{tot}$	$2.18 \times 10^{-3}$	$3.96 \times 10^{-3}$	$6.82 \times 10^{-3}$
$\xi_{int}$	$2.81 \times 10^{-2}$	$4.66 \times 10^{-2}$	$7.40 \times 10^{-2}$
$\xi_{ext}$	$1.01 \times 10^{-3}$	$2.29 \times 10^{-3}$	$3.84 \times 10^{-3}$
	$SNR = 10dB$		
	$IMSA - BCS$	$TVCS$	$BP$
$\xi_{tot}$	$2.05 \times 10^{-3}$	$4.34 \times 10^{-3}$	$9.04 \times 10^{-3}$
$\xi_{int}$	$2.29 \times 10^{-2}$	$4.67 \times 10^{-2}$	$7.40 \times 10^{-2}$
$\xi_{ext}$	$1.02 \times 10^{-3}$	$2.69 \times 10^{-3}$	$5.37 \times 10^{-3}$
	$SNR = 5dB$		
	$IMSA - BCS$	$TVCS$	$BP$
$\xi_{tot}$	$1.88 \times 10^{-3}$	$5.01 \times 10^{-3}$	$1.18 \times 10^{-2}$
$\xi_{int}$	$1.95 \times 10^{-2}$	$4.43 \times 10^{-2}$	$7.40 \times 10^{-2}$
$\xi_{ext}$	$9.40 \times 10^{-4}$	$3.48 \times 10^{-3}$	$7.32 \times 10^{-3}$

Table VII: *Rhombus*,  $D = 1.5\lambda$ ,  $\tau = 0.10$  - *IMSA-BCS* vs. *TVCS* vs. *BP* - Reconstruction errors: total ( $\xi_{tot}$ ), internal ( $\xi_{int}$ ) and external ( $\xi_{ext}$ ) errors.

#### 1.2.4 Rhombus, $D = 1.5\lambda$ , $\tau = 0.15$ - IMSA - BCS vs. TVCS vs. BP reconstructed profiles

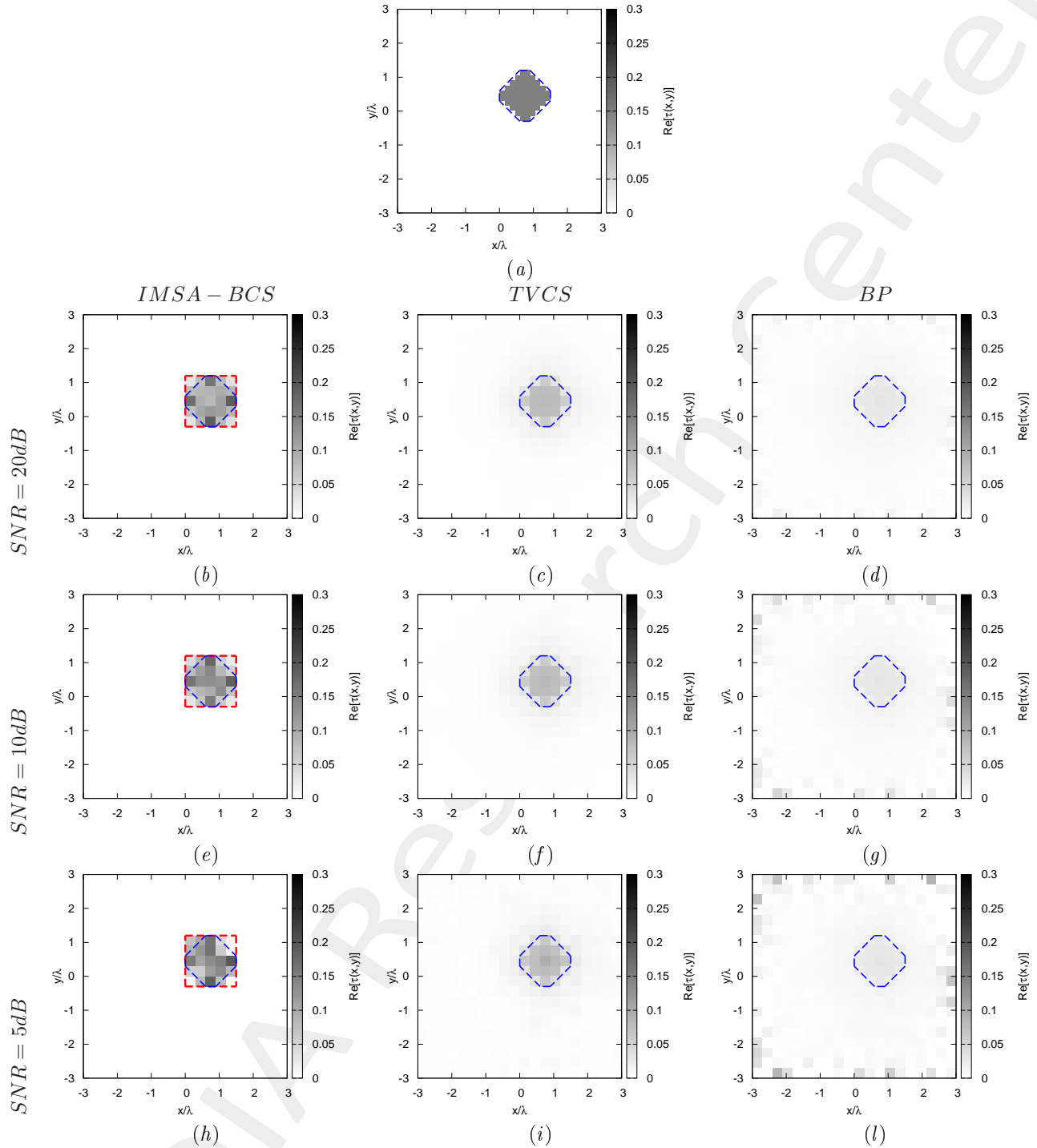


Figure 9: Rhombus,  $D = 1.5\lambda$ ,  $\tau = 0.15$  - IMSA-BCS vs. TVCS vs. BP - (a) Actual profile, (b)(e)(h) IMSA-BCS, (c)(f)(i) TVCS and (d)(g)(l) BP reconstructed profiles for (b)(c)(d)  $SNR = 20$  [dB], (e)(f)(g)  $SNR = 10$  [dB] and (h)(i)(l)  $SNR = 5$  [dB].

	$SNR = 50dB$		
	$IMSA - BCS$	$TVCS$	$BP$
$\xi_{tot}$	$3.51 \times 10^{-3}$	$6.20 \times 10^{-3}$	$9.17 \times 10^{-3}$
$\xi_{int}$	$4.27 \times 10^{-2}$	$7.17 \times 10^{-2}$	$1.07 \times 10^{-1}$
$\xi_{ext}$	$1.52 \times 10^{-3}$	$3.64 \times 10^{-3}$	$5.18 \times 10^{-3}$
	$SNR = 20dB$		
	$IMSA - BCS$	$TVCS$	$BP$
$\xi_{tot}$	$3.53 \times 10^{-3}$	$6.28 \times 10^{-3}$	$1.00 \times 10^{-2}$
$\xi_{int}$	$4.09 \times 10^{-2}$	$7.20 \times 10^{-2}$	$1.07 \times 10^{-1}$
$\xi_{ext}$	$1.62 \times 10^{-3}$	$3.71 \times 10^{-3}$	$5.65 \times 10^{-3}$
	$SNR = 10dB$		
	$IMSA - BCS$	$TVCS$	$BP$
$\xi_{tot}$	$3.06 \times 10^{-3}$	$6.76 \times 10^{-3}$	$1.33 \times 10^{-2}$
$\xi_{int}$	$3.18 \times 10^{-2}$	$7.19 \times 10^{-2}$	$1.07 \times 10^{-1}$
$\xi_{ext}$	$1.38 \times 10^{-3}$	$4.22 \times 10^{-3}$	$7.91 \times 10^{-3}$
	$SNR = 5dB$		
	$IMSA - BCS$	$TVCS$	$BP$
$\xi_{tot}$	$3.39 \times 10^{-3}$	$7.73 \times 10^{-3}$	$1.74 \times 10^{-2}$
$\xi_{int}$	$3.40 \times 10^{-2}$	$6.94 \times 10^{-2}$	$1.07 \times 10^{-1}$
$\xi_{ext}$	$1.32 \times 10^{-3}$	$5.33 \times 10^{-3}$	$1.08 \times 10^{-2}$

Table VIII: *Rhombus*,  $D = 1.5\lambda$ ,  $\tau = 0.15$  - *IMSA-BCS* vs. *TVCS* vs. *BP* - Reconstruction errors: total ( $\xi_{tot}$ ), internal ( $\xi_{int}$ ) and external ( $\xi_{ext}$ ) errors.

### 1.2.5 Rhombus, $D = 1.5\lambda$ , $\tau = 0.20$ - IMSA - BCS vs. TVCS vs. BP reconstructed profiles

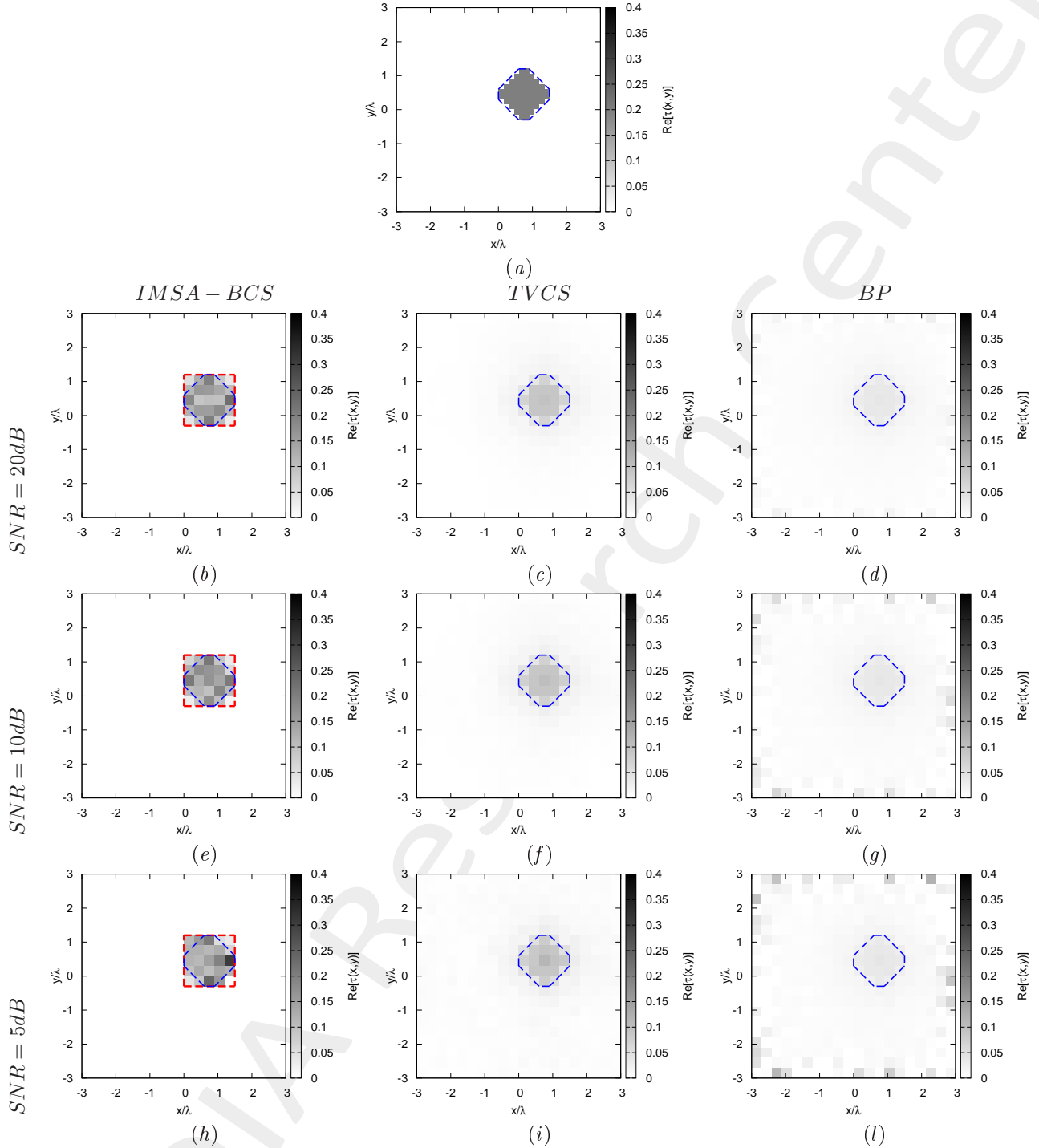


Figure 10: Rhombus,  $D = 1.5\lambda$ ,  $\tau = 0.20$  - IMSA-BCS vs. TVCS vs. BP - (a) Actual profile, (b)(e)(h) IMSA-BCS, (c)(f)(i) TVCS and (d)(g)(l) BP reconstructed profiles for (b)(c)(d) SNR = 20 [dB], (e)(f)(g) SNR = 10 [dB] and (h)(i)(l) SNR = 5 [dB].

	$SNR = 50dB$		
	$IMSA - BCS$	$TVCS$	$BP$
$\xi_{tot}$	$4.83 \times 10^{-3}$	$8.84 \times 10^{-3}$	$1.19 \times 10^{-2}$
$\xi_{int}$	$4.18 \times 10^{-2}$	$1.01 \times 10^{-1}$	$1.38 \times 10^{-1}$
$\xi_{ext}$	$2.16 \times 10^{-3}$	$5.25 \times 10^{-3}$	$6.69 \times 10^{-3}$
	$SNR = 20dB$		
	$IMSA - BCS$	$TVCS$	$BP$
$\xi_{tot}$	$4.86 \times 10^{-3}$	$8.86 \times 10^{-3}$	$1.31 \times 10^{-2}$
$\xi_{int}$	$4.42 \times 10^{-2}$	$1.01 \times 10^{-1}$	$1.38 \times 10^{-1}$
$\xi_{ext}$	$2.13 \times 10^{-3}$	$5.25 \times 10^{-3}$	$7.31 \times 10^{-3}$
	$SNR = 10dB$		
	$IMSA - BCS$	$TVCS$	$BP$
$\xi_{tot}$	$4.56 \times 10^{-3}$	$9.40 \times 10^{-3}$	$1.74 \times 10^{-2}$
$\xi_{int}$	$3.97 \times 10^{-2}$	$9.96 \times 10^{-2}$	$1.38 \times 10^{-1}$
$\xi_{ext}$	$1.95 \times 10^{-3}$	$5.89 \times 10^{-3}$	$1.03 \times 10^{-2}$
	$SNR = 5dB$		
	$IMSA - BCS$	$TVCS$	$BP$
$\xi_{tot}$	$5.47 \times 10^{-3}$	$1.07 \times 10^{-2}$	$2.28 \times 10^{-2}$
$\xi_{int}$	$5.71 \times 10^{-2}$	$9.75 \times 10^{-2}$	$1.38 \times 10^{-1}$
$\xi_{ext}$	$2.22 \times 10^{-3}$	$7.34 \times 10^{-3}$	$1.41 \times 10^{-2}$

Table IX: *Rhombus*,  $D = 1.5\lambda$ ,  $\tau = 0.20$  - *IMSA-BCS* vs. *TVCS* vs. *BP* - Reconstruction errors: total ( $\xi_{tot}$ ), internal ( $\xi_{int}$ ) and external ( $\xi_{ext}$ ) errors.

### 1.2.6 Rhombus, $D = 1.5\lambda$ - IMSA – BCS vs. TVCS vs. BP errors resume vs. $\tau$

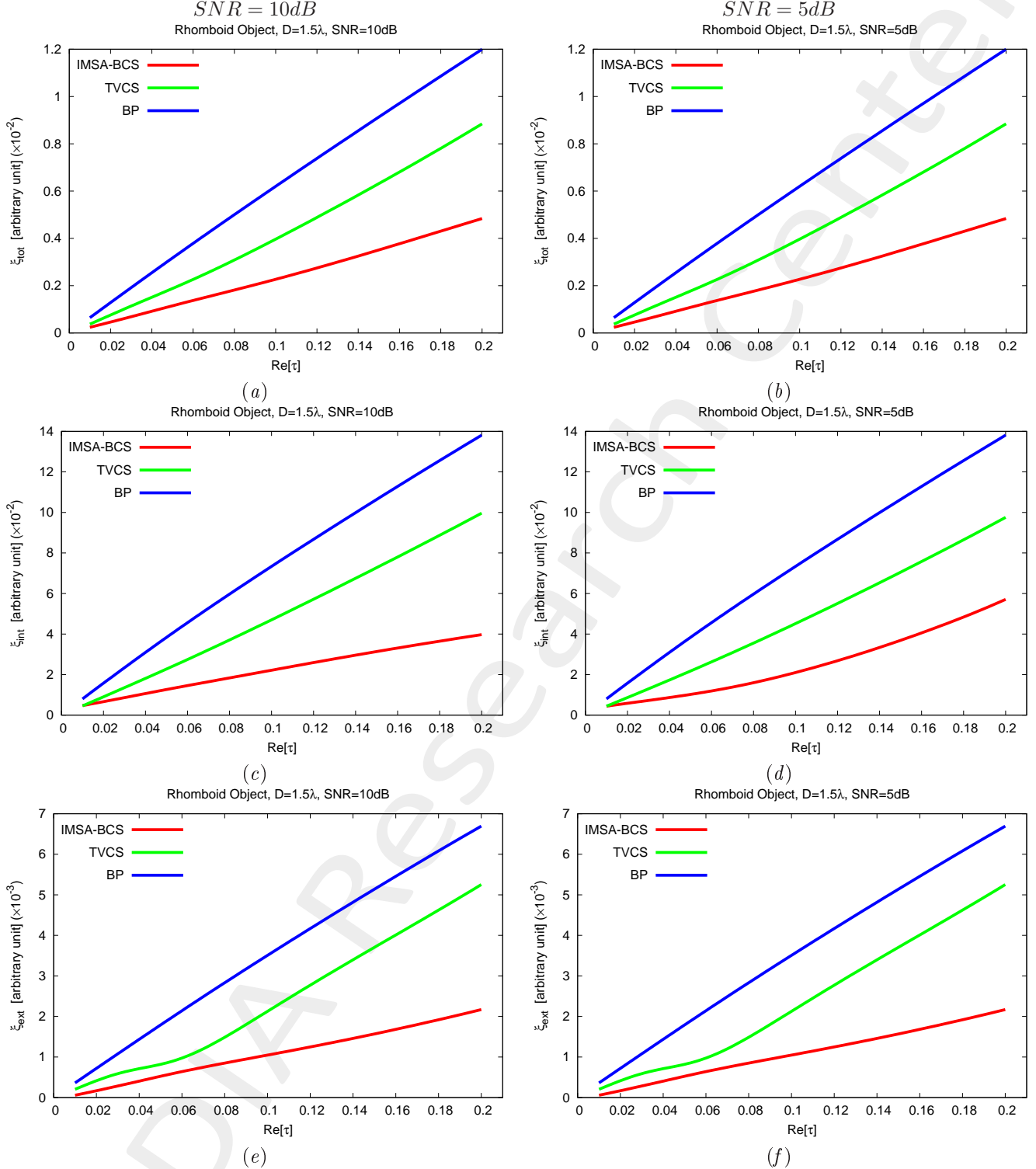


Figure 11: Rhombus,  $D = 1.5\lambda$  - Reconstruction errors vs.  $\tau$ : (a) total error, (b) internal error and (c) external error. Reconstruction errors vs.  $\tau$ : (a)(b) total error, (c)(d) internal error and (e)(f) external error for (a)(c)(e)  $\text{SNR} = 10\text{dB}$  and (b)(d)(f)  $\text{SNR} = 5\text{dB}$ .

---

**More information on the topics of this document can be found in the following list of references.**

## References

- [1] M. Salucci, G. Oliveri, and A. Massa, "GPR prospecting through an inverse scattering frequency-hopping multi-focusing approach," *IEEE Trans. Geosci. Remote Sens.*, vol. 53, no. 12, pp. 6573-6592, Dec. 2015.
- [2] M. Salucci, L. Poli, N. Anselmi, and A. Massa, "Multifrequency Particle Swarm Optimization for enhanced multi-resolution GPR microwave imaging," *IEEE Trans. Geosci. Remote Sens.*, vol. 55, no. 3, pp. 1305-1317, Mar. 2017.
- [3] M. Salucci, L. Poli, and A. Massa, "Advanced multi-frequency GPR data processing for non-linear deterministic imaging," *Signal Processing*, vol. 132, pp. 306-318, Mar. 2017.
- [4] N. Anselmi, G. Oliveri, M. Salucci, and A. Massa, "Wavelet-based compressive imaging of sparse targets," *IEEE Trans. Antennas Propag.*, vol. 63, no. 11, pp. 4889-4900, Nov. 2015.
- [5] G. Oliveri, M. Salucci, N. Anselmi, and A. Massa, "Compressive sensing as applied to inverse problems for imaging: theory, applications, current trends, and open challenges," *IEEE Antennas Propag. Mag.*, vol. 59, no. 5, pp. 34-46, Oct. 2017.
- [6] A. Massa, P. Rocca, and G. Oliveri, "Compressive sensing in electromagnetics - A review," *IEEE Antennas Propag. Mag.*, pp. 224-238, vol. 57, no. 1, Feb. 2015.
- [7] N. Anselmi, L. Poli, G. Oliveri, and A. Massa, "Iterative multi-resolution bayesian CS for microwave imaging," *IEEE Trans. Antennas Propag.*, vol. 66, no. 7, pp. 3665-3677, Jul. 2018.
- [8] N. Anselmi, G. Oliveri, M. A. Hannan, M. Salucci, and A. Massa, "Color compressive sensing imaging of arbitrary-shaped scatterers," *IEEE Trans. Microw. Theory Techn.*, vol. 65, no. 6, pp. 1986-1999, Jun. 2017.
- [9] G. Oliveri, N. Anselmi, and A. Massa, "Compressive sensing imaging of non-sparse 2D scatterers by a total-variation approach within the Born approximation," *IEEE Trans. Antennas Propag.*, vol. 62, no. 10, pp. 5157-5170, Oct. 2014.
- [10] L. Poli, G. Oliveri, and A. Massa, "Imaging sparse metallic cylinders through a local shape function Bayesian compressive sensing approach," *J. Opt. Soc. Am. A*, vol. 30, no. 6, pp. 1261-1272, 2013.
- [11] L. Poli, G. Oliveri, F. Viani, and A. Massa, "MT-BCS-based microwave imaging approach through minimum-norm current expansion," *IEEE Trans. Antennas Propag.*, vol. 61, no. 9, pp. 4722-4732, Sep. 2013.
- [12] F. Viani, L. Poli, G. Oliveri, F. Robol, and A. Massa, "Sparse scatterers imaging through approximated multitask compressive sensing strategies," *Microwave Opt. Technol. Lett.*, vol. 55, no. 7, pp. 1553-1558, Jul. 2013.
- [13] L. Poli, G. Oliveri, P. Rocca, and A. Massa, "Bayesian compressive sensing approaches for the reconstruction of two-dimensional sparse scatterers under TE illumination," *IEEE Trans. Geosci. Remote Sens.*, vol. 51, no. 5, pp. 2920-2936, May 2013.

- 
- [14] L. Poli, G. Oliveri, and A. Massa, "Microwave imaging within the first-order Born approximation by means of the contrast-field Bayesian compressive sensing," *IEEE Trans. Antennas Propag.*, vol. 60, no. 6, pp. 2865-2879, Jun. 2012.
  - [15] G. Oliveri, L. Poli, P. Rocca, and A. Massa, "Bayesian compressive optical imaging within the Rytov approximation," *Optics Letters*, vol. 37, no. 10, pp. 1760-1762, 2012.
  - [16] G. Oliveri, P. Rocca, and A. Massa, "A Bayesian compressive sampling-based inversion for imaging sparse scatterers," *IEEE Trans. Geosci. Remote Sens.*, vol. 49, no. 10, pp. 3993-4006, Oct. 2011.
  - [17] G. Oliveri, M. Salucci, and N. Anselmi, "Tomographic imaging of sparse low-contrast targets in harsh environments through matrix completion," *IEEE Trans. Microw. Theory Tech.*, vol. 66, no. 6, pp. 2714-2730, Jun. 2018.
  - [18] M. Salucci, A. Gelmini, L. Poli, G. Oliveri, and A. Massa, "Progressive compressive sensing for exploiting frequency-diversity in GPR imaging," *J. Electromagn. Waves Appl.*, vol. 32, no. 9, pp. 1164- 1193, 2018.